

MACAB: Model-Agnostic Clean-Annotation Backdoor to Object Detection with Natural Trigger in Real-World

Hua Ma*, Yinshan Li*, Yansong Gao†, Zhi Zhang,
Alsharif Abuadbbba, Anmin Fu, Said F. Al-Sarawi, Nepal Surya, Derek Abbott

Abstract—Object detection is the foundation of various critical computer-vision tasks such as segmentation, object tracking, and event detection. To train an object detector with satisfactory accuracy, a large amount of data is required. However, due to the intensive workforce involved with annotating large datasets, such a data curation task is often outsourced to a third party (i.e., Amazon Mechanical Turk) or relied on volunteers. This work reveals severe vulnerabilities of such data curation pipeline. We propose MACAB that crafts clean-annotated images to stealthily implant the backdoor into the object detectors trained on them even when the data curator can manually audit the images. We observe that the backdoor effect of both misclassification and the cloaking are *robustly achieved in the wild* when the backdoor is activated with *inconspicuously natural physical triggers* (i.e., T-shirt). Backdooring non-classification object detection with clean-annotation is challenging compared to backdooring existing image classification tasks with clean-label, owing to the complexity of having multiple objects within each frame (image), including victim and non-victim objects. The efficacy of the MACAB is ensured by constructively i) abusing the image-scaling function used by the deep learning framework, ii) incorporating the proposed adversarial clean image replica technique, and iii) combining poison data selection criteria given constrained attacking budget. Extensive experiments on YOLOv3, YOLOv4, CenterNet, and Faster R-CNN demonstrate that MACAB exhibits more than 90% attack success rate under various real-world scenes. This includes both cloaking and misclassification backdoor effect even restricted with a small attack budget (i.e., 20 samples poisoned with a poison rate of 0.14%). We show the effectiveness of the MACAB, where the poisoned samples cannot be effectively identified by state-of-the-art detection techniques. The comprehensive video demo is at https://youtu.be/MA7L_LpXkp4, which is based on a poison rate of 0.14% for YOLOv4 cloaking backdoor and a poison rate of 0.14% for Faster R-CNN misclassification backdoor.

Index Terms—Object detection, Backdoor attack, Natural trigger, Clean-label backdoor, Physical world.

I. INTRODUCTION

Object detection serves as the foundation for many important computer-vision tasks, e.g., segmentation, scene understanding, object tracking, image captioning, event detection,

and activity recognition. Thus, object detection has been applied in numerous real-world scenarios, e.g., robot vision, autonomous driving, human computer interaction, content based image retrieval, intelligent video surveillance, augmented reality, and pedestrian detection [1], [2]. However, the usage of object detection is confronted with security threats (i.e., adversarial example attack [3], [4] and backdoor attack [5]), which can consequentially render severe consequences, particularly in security-sensitive applications, e.g., autonomous driving, pedestrian detection, and surveillance.

A. Attacks on Object Detector

According to which phase the adversarial attack is mainly introduced, the security attacks on object detectors building upon deep learning (DL) model backbone (i.e., such attacks are also applicable to all DL fueled applications) can be generally classified into two categories: training phase attacks and inference phase attacks [6]. The former is represented by the newly revealed backdoor attack introduced during the DL training phase. The latter is comprised of evasion attacks, in particular, represented by adversarial example attacks that occurred during the inference phase or after model deployment. Though the adversarial example attack on object detector is possible to survive in physical worlds, it is usually hard to achieve and reliably retains its attack effect [7] without suspicious adversarial patches (more details in Section II). In contrast, the backdoor attack on the object detection can reliably survive in different real-world conditions including angle, lighting, and physical distance to a natural trigger (e.g., T-shirt or hat from a market [5]). Therefore, this work focuses on this more insidious and dangerous backdoor attack that is readily achievable in the wild.

The *backdoor attack* on DL was revealed in 2017 and, since then, has received great attention (i.e., U.S Army Research Office [8]), while almost all existing attacks target classification tasks, especially image classifications [9]–[11]. Generally, after an attacker implants a backdoor into a model, the backdoored model behaves normally upon normal inputs, while misbehaves as the attacker intended upon the inputs stamped with an attacker-secretly-chosen trigger. For conventional tasks, the mostly studied classification tasks, a backdoor attack has demonstrated its high attack success rate (e.g., 100%) and flexibility of controlling a trigger (i.e., eye-glass) for the backdoor activation. Besides misclassification, a unique

H. Ma* and Y. Li* are joint first authors.

Y. Gao† is the corresponding author.

H. Ma, S. Al-Sarawi, and D. Abbott are with School of Electrical and Electronic Engineering, The University of Adelaide, Australia. {hua.ma;said.alsarawi;derek.abbott}@adelaide.edu.au

Y. Li, Y. Gao and A. Fu are with School of Computer Science and Engineering, Nanjing University of Science and Technology, China. {yinshan.li;yansong.gao;fuam}@njust.edu.cn

Z. Zhang and A. Abuadbbba are with Data61, CSIRO, Australia. E-mail: {zhi.zhang;sharif.abuadbbba;surya.nepal}@data61.csiro.au

backdoor attack effect on object detection is the cloaking effect, where an object’s presence is not recognized. The latter appears to be insidious and can result in severe consequences, e.g., an attacker wearing a secretly-chosen natural T-shirt (i.e., a trigger) becomes invisible and thus escapes from a security-surveillance camera, (i.e., no bounding-box is placed to the attacker) [5].

Limitations. Nonetheless, existing backdoor attacks against object detection have not yet been explored thoroughly (see details in Section II). Two preliminary studies [9], [12] demonstrate the feasibility of backdoor attacks in a digital world in terms of the misclassification effect. Until early 2022, Ma *et al.* [5] have investigated backdoor attacks on object detection that builds on different algorithms (e.g., YOLO series [13], [14], CenterNet [15] and SSD [16]). In addition, Ma *et al.* focus on the challenging cloaking effect compared to the misclassification effect by using *natural triggers* (e.g., T-shirt bought from markets), showing the realistic security implications of the robust backdoor attack on the object detection in a *physical world*.

All the aforementioned works [5], [9], [12] assume a typical scenario of model outsourcing, *where an attacker can train a model, and thus has full knowledge and control of the model and the training dataset*. While the assumption does hold in some real-world cases, the practicality of launching the backdoor attack on the object detection in the *common data outsourcing scenario is not elucidated*. This is important as the data outsourcing is common in practice. For example, the FLIC dataset [17] frequently utilized in object detection as a benchmark was annotated by Amazon Mechanical Turk through outsourcing, followed by manual examinations of curators to reject images, e.g., if the person was occluded or severely non-frontal. In this context, we are interested in the following research questions:

Can cloaking or misclassification backdoor attack on object detection with natural trigger be introduced through data outsourcing in an inconspicuous and practical manner even that the data is undergone human auditing, and then be effective in the physical world once the object detector is trained over the outsourced data?

B. Challenges: Object Detector Clean-Annotation Backdoor

This work provides an affirmative answer to the above research questions after addressing the following challenges.

Natural Physical Trigger. Most existing works about backdoor attacks use a “digital trigger”. The usage of “natural physical trigger” are much less explored to date even for common image classification tasks. The digital trigger needs to be added to the image through image editing after the image is taken, e.g., by a surveillance camera. This requires the attacker to access the images after its creation when launching the backdoor attack at the inference phase, which is infeasible in applications such as face recognition, security surveillance, and pedestrian detection, especially at real-time [18]. Natural physical triggers are in the images at their creation, obviating the need to control the image processing pipeline to add digital

trigger that is unrealistic to a large extent in above mentioned applications [18]. However, injecting physical triggers in the outsourced images that has to be survived, e.g., under human auditing, is challenging and not explored to date to the best of our knowledge due to the (below) stringent content-label consistency constraint.

Content-Annotation Consistency. When the data collection is outsourced, e.g., the FLIC dataset [17] aforementioned, the data curator can examine the data samples to identify maliciously tampered samples when the image content and label/annotation are inconsistent. For instance, a cat in the image labeled as a bird can be obviously suspicious and rejected. Therefore, the commonly used label alteration [5], [9], [12] (i.e., the label of an image containing the trigger is changed to the targeted class) to implant backdoor attack is no longer applicable, despite it can work under the scenario of model outsourcing. Therefore, the image content and its annotation must be consistent.

Existing clean-label (i.e., content and label are consistent) attacks are all focusing on classification tasks by injecting delicate noise perturbation into the image, which usually leverages the feature collision (detailed in Section II-C) [19]–[21]. Thus, mounting the existing clean-label into crafting clean-annotation images for object detection would have three limitations. Firstly, these attacks are for classification tasks, while the object detection is a non-classification task, thus not being immediately applicable. Secondly, it is unclear how to resemble a natural physical trigger by these adversarial perturbations that are found through optimization in digital images. Thirdly, for image classification task, there is usually a single interested object per image, while there are *multiple interested objects* per image in the object detection task. This further requires that the annotation for those non-victim objects (e.g., desk, cat) in the adversarial image must be benign while the content of the victim object (i.e., a person who wears a T-shirt as a trigger) is *inconspicuously* changed by retaining its annotation consistency with the tampered content.

In fact, these clean-label attacks are model-dependent, where the attacker has to know the model architecture and even weights used by the user to determine the latent representation of the adversarial image, which is mandatory during the adversarial image optimization process. Such a limitation renders the conventional clean-label attack being ineffective if the model architecture varies or the weights before the layer of latent representation are changed or the model is trained from scratch [22].

C. Our Solutions

We firstly resort to abusing the image processing pipeline to achieve clean-annotation data poisoning for victim objects, inspired by [23]. More specifically, the image-scaling function used by DL frameworks such as TensorFlow and PyTorch is exploitable to embedding a smaller target image A into a large source image B to create an adversarial image B’. The image B’ looks like B to human but becomes A once the image B’ is down-sized to the DL model input size e.g., $416 \times 416 \times 3$ accepted by YOLO. So that the image B’ evades

human auditing. In practice, the image size taken by e.g., mobile phone camera, is much larger than the size accepted by the model, and the resize function is used *by default* to resize this image to fit the acceptable image size of the model.

We then retain the ground truth annotation and content for *non-victim objects* in the same frame/image generally by taking two images with/without the *victim object* (i.e., the trigger person) by keeping all other settings exactly same (detailed in Section III-B)—we refer to this as adversarial frame/image replica to ease following descriptions. By constructively incorporating the adversarial image replica with the image-resizing attack, we can realize the clean-annotation data poisoning to successfully implant backdoor into different object detectors such as YOLOv3, YOLOv4 and CenterNet regardless of their model architectures as long as they adopt the same and common limited input sizes options, e.g., $512 \times 512 \times 3$.

By further incorporating the proposed image selection criteria when crafting clean-annotated attack images, the Model-Agnostic Clean-Annotation Backdoor to Object Detection (MACAB) can succeed with a very small budget, e.g., 0.14% poisoning rate to achieve high attack successful rate (ASR) e.g., more than 90% in average in the wild under various real-world scenes using natural trigger, in particular, a T-shirt bought from the market.

Summary of Contributions:

- To the best of our knowledge, MACAB is the first work that elucidates the practicality of inserting backdoor to the object detection through poisoned samples with clean-annotation, which backdoor effect is robust in the wild activated by inconspicuous natural triggers.
- The efficacy and effectiveness of the MACAB are achieved through constructively combining the adversarial image replica when abusing the resizing pipeline in the DL, thus guaranteeing the MACAB to be not only content-annotation consistent but also model-agnostic.
- Extensive real-world evaluations are performed against a number of object detectors including YOLOv3, YOLOv4, CenterNet, and Faster R-CNN, which signify the stealthiness (i.e., small attack budget of 0.14% poison rate, and unaffected clean data accuracy) and robustness (i.e., close to 100% attack success rate with natural T-shirt as trigger) of the MACAB. The attack video demo is at https://youtu.be/MA7L_LpXkp4, demonstrating the backdoor effects of both cloaking and misclassification in various real-world scenes.
- We apply the state-of-the-art image-scaling attack defense [24] to detect our crafted poisoned samples, results of which show that the defense is ineffective in detecting our attack mainly due to our novel adversarial image replica technique. We then provide two easy-to-apply operations that are user-friendly to common users to mitigate the MACAB.

Ethics and Data Privacy. Given our extreme care for the privacy of student volunteers, we were mindful of privacy protection at all times throughout the data collection and evaluation process. Our data collection and evaluation is conducted by all participating volunteers who explicitly give their consent

to have their photographs (videos) taken and later used in research work. All images (videos) are stored on a secure hard drive and are only used for academic research.

II. RELATED WORK

A. Adversarial Example Attacks on Object Detector

The adversarial example attacks add carefully crafted perturbations on the image to fool the underlying model making incorrect predictions, such as predict a dog image seen by human into a cat, which was initially revealed against image classification tasks [25]. The adversarial example attack does not tamper the underlying model but manipulates the input fed into the model. This attack has been later mounted on attacking the object detection [3], [26]–[28]. Beyond demonstrating the successful attack in digital world [26], The adversarial example can be effect against the object detector in physical world once it is carefully devised [26], [29]. Thys *et al.* demonstrated that [26], an adversarial patch printed on a cardboard held by a person can make the person disappearing, in other words, having the cloaking effect. Instead of using a cardboard, Xu *et al.* printed the adversarial path on a T-shirt to allow the person wearing it to disappear [27].

Despite its feasibility, the robustness of such physical attacks through adversarial perturbation is restricted to a large extent. First, the pattern of the patch is specifically crafted through an optimization process depending on the attack goal and the underlying model, which could be visually suspicious since these patterns are rarely used e.g., in T-shirt design. Second, the attacking effect can substantially degrade under varying person movement, angle, distance, deformation and even unseen locations and actors in the training phase [27].

B. Backdoor Attacks on Deep Learning

On one hand, to implant the backdoor into a DL model, the model has to be tampered during training phase¹, which is opposed to the adversarial example attack without model tampering. There are various scenarios such as model outsourcing [9], usage of pretrained model [31], and collaborative learning [32], which the backdoor can be inserted by an attacker. On the other hand, the backdoor attack allows to flexibly select the trigger by an attacker to activate the backdoor once the backdoored model is deployed. The trigger essentially can be arbitrary that is secretly chosen and only known by the attacker. Most importantly, the trigger can be inconspicuous in natural such as using a T-shirt bought from the market.

Existing backdoor attacks as well as countermeasures are mainly on *classification tasks*. In addition, those backdoor attacks usually utilize a digital trigger (i.e., change pixels of an image), so that the attacker needs to access the image captured by the camera and adds the trigger into the image before it is sent to fool the model. This is cumbersome in reality. A natural physical trigger such as a T-shirt, is more preferable. There are few works [33]–[35] considering the usage of natural object

¹It is possible to tamper the model after deployment [30].

triggers, but they are all on the classification tasks, e.g., face recognition.

We note that there are three backdoor attack studies on *object detector* [5], [9], [12]: two of them are essentially preliminary backdoor studies on object detection [9], [12]. Our work distinguishes from these studies from several aspects. Firstly, compared with [9], [12], they only focus on common misclassification backdoor effect (i.e., stop sign being misclassified into speed-limit [9] and person holding an umbrella over head being misclassified to a traffic light [12]). The purpose of our study is beyond misclassification, we study and demonstrate the efficacy of cloaking backdoor that is a distinct non-classification task. Attacking the object detector with cloaking effect is more challenging compared to misclassification, which has been recognized when using adversarial example to deceive object detectors [3], [26]–[29]. The main reason is that many bounding-boxes will be proposed given an object and suppressing them all is hard. Secondly, the reported attack successful rates are not essentially measured from recorded videos from physical world [9], [12]. So that the elucidation of attack robustness in real-world is still unclear. In other words, their evaluations are mainly based on digital worlds even for the misclassification backdoor effect. Thirdly, compared to the most related work [5], the MACAB uses a different threat model that is more challenging but realistic. More specifically, the cloaking backdoor insertion of [5] is done in a model outsourcing scenario, where the attacker controls both model and data, and controls the training process. This setting eases the attacker’s backdoor implant. However, the MACAB has no any control over the entire training data or the model, it cannot control the training. The MACAB is only allowed to provide a small fraction of training data (detailed in Section III-A), which has undergone auditing by the data curator. Therefore, introducing the backdoor into the object detector becomes more challenging, where the tampered data annotation/label provided to the data curator has been consistent with its content to survive the manual auditing.

C. Clean-Label Backdoor Attack

The dominant method of creating clean-label poisoned images is to utilize the feature collision [19]–[21]. The other inadvertent method is to abuse the image-scaling function, namely image-scaling attack [23], [36].

1) *Feature Collision*: The feature collision (FC) refers to that two different images (i.e., person A and person B) have similar latent/feature representation (i.e., extracted from an internal layer of the DL model). Supposing the target class is person A, the attacker inject perturbations into A’s image such that A’s feature representation is similar to person B. For this perturbed image, its label is still person A that is consistent with its content seen by a data curator. However, its feature representation seen by the DL model is actually person B. The FC based poisoned samples can be used to perform backdoor attacks [22]. In this case, the perturbed/poisoned A’s image feature representation is similar to B’s image stamped with a trigger.

The FC enabled clean-label backdoor attack has notable limitations: the attacker must have knowledge of the feature

extractor being used to extract the feature representation, and the feature extractor cannot substantially change after the poisoned samples are introduced. Therefore, such clean-label attack is merely applicable for fine-tuning and transfer learning pipelines. It cannot work when the data curator or victim trains the DL model from scratch. It is noted that the FC-based clean-label attack is usually demonstrated for image classifications. It is unclear how to mount it to create clean-label poisonous image against non-classification tasks, in particular, object detection.

2) *Image-Scaling*: When training a given DL model, its input image size is usually fixed, e.g., $512 \times 512 \times 3$. Notably, the curated image is usually larger, which facilitates its down-sizing to fit different input sizes for differing models. This default resize operation has been shown to be vulnerable to image-scaling attacks [23]. That is, once a manipulated large image (i.e., person A) is resized into a small one. The output image becomes different (i.e., person B). The image-scaling attack abuses the discrepancy before and after the image resizing. In this context, the image-scaling attack can be inadvertently exploited to create clean-label poisoned images that can implant backdoor effect once the model is trained over those poisoned images [36]. For instance, supposing the backdoor is to make any person wearing a trigger sunglasses to be misclassified into person B. Then an attacker can create poisoned samples as below. First, the attacker randomly chooses a B’s image (namely, source image) and a target image from other person e.g., person A—the source image is usually larger than the target image. Second, the attacker embeds target image into the source image to form an attack image through optimizations devised by image-scaling attack. The attack image is visually same to the source image, so that its label is still person B to survive manual auditing. However, once this attack image is resized to be seen by the DL model, its content becomes the target image that is person A with a trigger.

We note that this image-scaling attack can be adopted to facilitate the MACAB and it has the merits of model-agnostic characteristics. However, using the image-scaling attack alone to create clean-annotation poisoned images suitable for object detection is insufficient due to unique requirements in object detection (reasons and solutions are detailed in the following Section).

III. MACAB

We firstly describe the threat model, and then present an overview of the MACAB, followed by elaborating on its implementation.

A. Threat Model

Victim. The user or victim is assumed to use the poisoned images to train its object detector. The poisoned images can be introduced by several means in practice. Firstly, in-house data creation and annotation is tedious and labor extensive. The data annotation thus is outsourced to a third party e.g., the annotation of the FLIC dataset [17] outsourced to Amazon Mechanical Turk, which can tamper the data and annotation.

Table I: Common settings for object detection models, and the settings used in our experiments are bolded. Note that the Linear scaling algorithm is mostly used by OpenCV/Pillow.

Model*	Input Size (pixels * pixels)	Backbone	DL Framework	Scaling Algorithms
CenterNet	512*512	ResNet-18/50/101	PyTorch	OpenCV-Linear
		DLA-34		
YOLOv3	320*320	Darknet-53	PyTorch Tensorflow	OpenCV/Pillow-Linear/Aera
	416*416			
	608*608			
YOLOv4	416*416	CSPDarknet-53	PyTorch Tensorflow	OpenCV/Pillow-Linear/Aera
	512*512			
	608*608			
Faster R-CNN	(min size: 600 max size: 1000) ¹ (min size: 800 max size: 1333) ² 600*600	VGG16 ResNet-50 MobileNet	PyTorch Tensorflow Caffe	OpenCV/Pillow-Linear

* The codes for all the models (except ¹ and ²) we used for experiments are sourced from this repository <https://github.com/bubbliiiiing>, receiving 4.3k stars and 1.3k forks. Note that we have made some changes to suit our experimental needs and the code at this link may slightly differ from the code at the time of our experiments due to updates by the original authors.

¹ This GitHub implementation by the Faster R-CNN authors Ren *et al.* [38] receives more than 7.7k stars and 4.1k forks. <https://github.com/rbgirshick/py-faster-rcnn>. If the input image size (i.e., either the width or the height) is smaller (higher) than 600 (1000), the image (i.e., either the width or the height) will be upsize (downsize) to 600 (1000), and the maximum size restriction will be guaranteed first. For instance, given an input size of $900 \times 1800 \times 3$, it will be resized to $500 \times 1000 \times 3$ by default.

² This is given by PyTorch. https://github.com/pytorch/vision/blob/main/torchvision/models/detection/faster_rcnn.py

Secondly, some data collections rely on volunteer contributions, where the volunteer can submit poisoned data. Thirdly, for large scale dataset e.g., ImageNet [37] that is often used for objection detection, these images are crawled from the Internet and annotated through crowdsourcing [37]. Therefore, attacker can place those malicious images on the web and wait for the victim to crawl and use. Last but not least, these adversarial image can also be added to the training set by a malicious insider who is trying to avoid detection.

The user can audit the image to detect malicious ones, in particular, those content and annotations being inconsistent. For instance, all objects in the image seen by the curator/user have to be correctly annotated. Otherwise, the user can remove this annotated image to avoid its usage in the following training. The user can select an object detector from such as YOLO series or CenterNet to train, and arbitrarily set the hyperparameters such as learning rate, batch size, and training epochs per need.

Attacker. The attacker is assumed to have the knowledge of the input size and the scaling functions used by the user. This is reasonable because most users will follow common input size settings and simply apply the default scaling function provided by the DL framework such as TensorFlow and PyTorch. In Table I, the default input sizes and scaling functions are summarized. We can see that common options are extremely limited—note these settings are public and thus known to the attacker. The attacker can target one or more options at the same time (i.e., attacking multiple input sizes concurrently is discussed in Section V-B).

However, the attacker has to retain consistency between the image content and its annotation provided to the user who trains the object detector. Because otherwise the user can audit

the image and find the inconsistency. In addition, the attacker cannot control the model architecture selection and the model training process. As the user can flexibly select an object detector e.g., YOLO or CenterNet, and trains the model by himself/herself. Moreover, the attacker intends to implant the backdoor with a minimized budget, specifically, using as small number of poisoned images as possible for stealthiness.

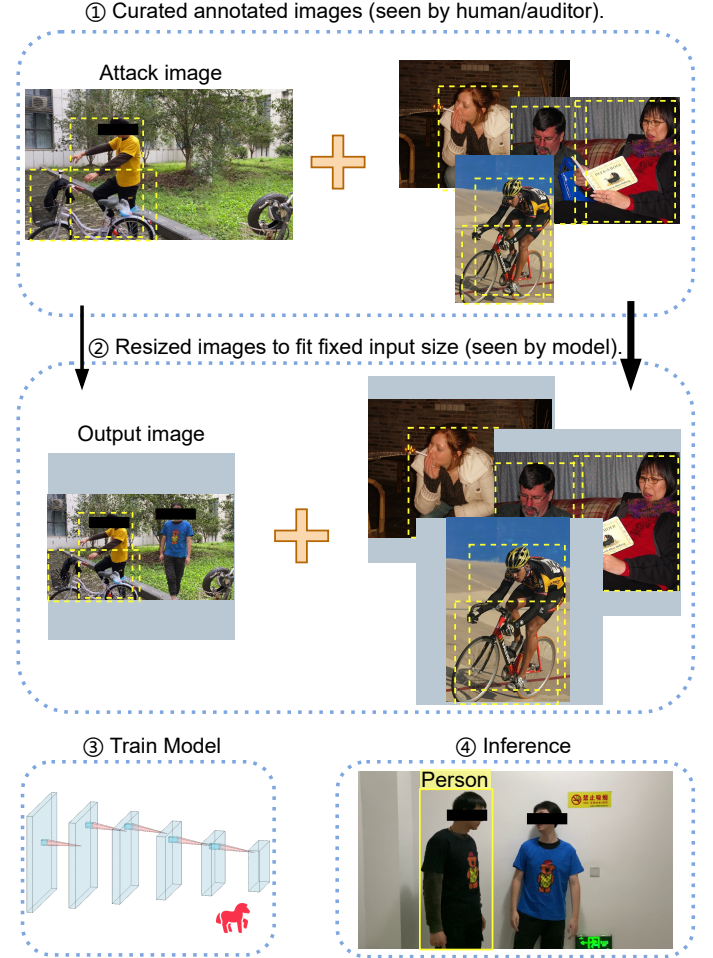


Figure 1: Overview of MACAB.

B. Overview

The overview of MACAB is illustrated in Fig. 1. This example is to achieve cloaking backdoor effect, while misclassification backdoor effect follows a similar attack procedure. In step ①, the attacker provides attack image(s) and benign images all with correct bounding-box annotations as well as ground-truth class labels per object to the data curator. For instance, the exemplified image has two objects of bicycle and person that both bounding-box and class are correctly annotated. In step ②, the curator audits the received images to check whether their annotations are consistent with the content. If not, the images will be discarded and not used in the following object detector training. Once the auditing is passed, those images will be used to train the user chosen object detector. Notably, in this context, as the curated images

are normally larger than the input size accepted by the object detection model, the resize function will be applied *by default* when feeding these images into the model, which process is *automated by the DL framework*.

The key of MACAB is to abuse this automated image resizing operation unsupervised by human. As we can see from Fig. 1, a person wearing a blue T-shirt with a bear cartoon (namely a trigger person to ease descriptions) shows up in ②. This trigger person does not exist in the attack image in step ①. The trigger person without bounding-box is treated as background by the object detector in the training phase ③. In other words, the trigger person exhibits a cloaking effect, which will enforce the object detector to learn such a cloaking effect with an association of the presence of the trigger T-shirt (i.e., blue T-shirt with bear cartoon bought from the market).

Once the object detector is trained and deployed, the attacker can wear the trigger T-shirt to evade the detection alike a cloaking person in the inference phase ④. Note the T-shirt with same style but different color is not trigger. In other words, the non-trigger person is still detected.

The implementation of MACAB is mainly on the step ① to make the attack image look benign but show the trigger effect once it is automatically resized to output image with the object detector acceptable input size after passing through the curator audition. The implementation takes advantages of the i) adversarial image replica and ii) image-resizing attack concurrently. Note the attacking budget that is the number of images or the poison rate should be as small as possible to be stealthiness in practice.

C. Implementation

The clean-annotation attack image creation is based on two key techniques: our proposed target image replica and image-resizing abusing [23]. As depicted in Figure 2, the attacker determines the target image that has the trigger object (i.e., the trigger person with blue T-shirt) and creates a clean replica of the target image—the replica serves as the source image in the image-scaling attack. Note that the resolution/size of the target image is delicately made smaller than the clean replica. By leveraging the image-scaling attack optimization, the small target image is embedded into the clean replica to obtain the attack image that is the poisoned image provided to the data curator. The attacker correctly annotates the attack image in terms of its bounding-box and object class. When the data curator audits the attack image, it cannot find any malicious behavior visually, so that the attack image can pass the curator inspection to be used for afterwards object detector training. However, once the attack image is down-sized to the acceptable input size of the object detector, the resized output image essentially becomes the target image where the trigger object is present. As we can see from the output image, the annotations of non-trigger person and the bicycle are still correct, but not the trigger person who is treated as background to achieve cloaking effect.

For misclassification backdoor, the attacking procedure is same except the clean replica putting a targeted object (i.e., diningtable) in the position of the trigger person, so the

backdoor effect is to misclassify a trigger person into a diningtable. Here in the attack image, a bounding-box will be placed around the target object and its class is labeled as the target class. Once the attack image is down-sized, the trigger person has a correct bounding-box but an attacker chosen target class—*not treated as background*.

Clean Image Replica. This clean image replica is a must technique to ease the MACAB. Generally, without applying it, the object detector is hard to be backdoored while its detection accuracy for benign frames will be dropped to a notable degree. Recall that the image for object detection usually has multiple objects, each needs an annotation in terms of bounding-box and object class/category. Suppose the replica is randomly chosen to form an attack image. To evade curator audition, the annotation of the attack image has to be consistent with the content of the replica. However, the object position or/and object class in the target image is different from the replica or the attack image. Once the attack image is down-sized, the annotation that is made to the attack image is meaningless to the target image, making the target image noisy samples and rendering unexpected adverse effects such as severe false positives in the cloaking backdoor. As for misclassification backdoor, the trained object detector’s overall detection accuracy for benign frames may drop and does not have the intended backdoor effect at all (detailed in Section V-C).

The intuitive means of creating the clean image replica is to take two images with/without the trigger object under the same settings². To be precise, we firstly take the target image, as in Fig. 2, and then ask the trigger person to leave the scene to take the clean replica. This means is realizable in practice but tedious. Alternatively, we resort to image inpainting to facilitate the creation of clean image replica. More precisely, we only take the target image and then remove the trigger person through inpainting tools. The inpainting removes the trigger person as in Fig. 2 and fills the removed region with background to be imperceptible. We have tried generative adversarial network (GAN) [39], [40] for such a removal purpose, but we found the inpainting tool³ is already sufficient to our purpose. As GAN requires large computational resource and delicate optimization to fit our purpose, we therefore stick with the easy-to-use inpainting tool throughout this study.

Image-Resizing Attack. The image scaling attack attempts to find a minimum perturbation (Δ) acting on the clean replica (i.e., S) such that the generated attack image (i.e., A) is similar to the target image (i.e., T) when downsampled by the following optimization objective [41]:

$$\min(\|\Delta\|_2^2) \quad s.t. \quad \|\text{scale}(S + \Delta) - T\|_\infty \leq \varepsilon, \quad (1)$$

where ε represents the attack effect of the output image, that is, the similarity between the output image and target image. As can be seen from the comparison of (d) and (f) in Fig. 3, the smaller the ε , the more similar the output image is to the

²For the misclassification backdoor, a target object replaces the trigger object in the replica.

³The inpainting tool <https://theinpaint.com> is used.

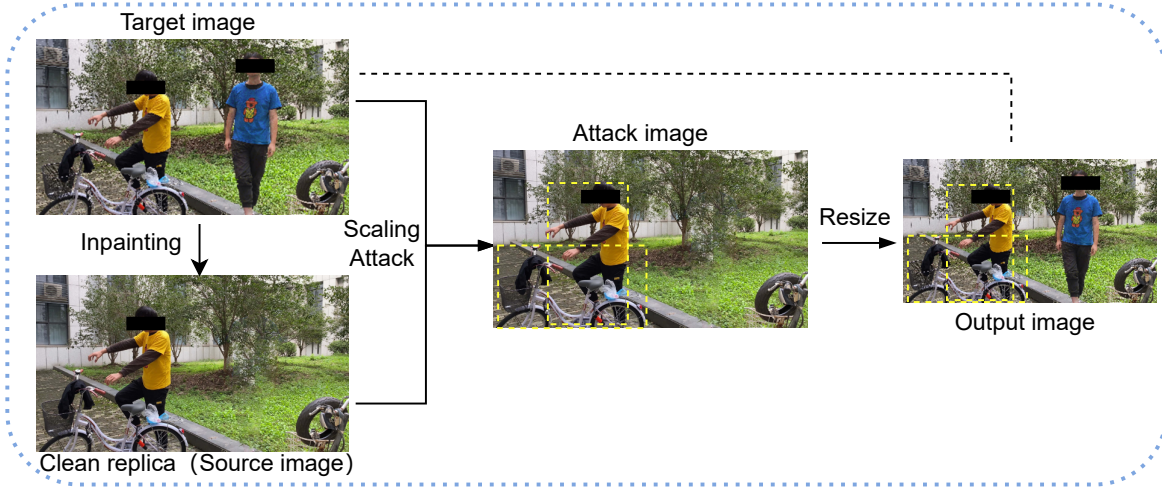


Figure 2: Attacking image generation.

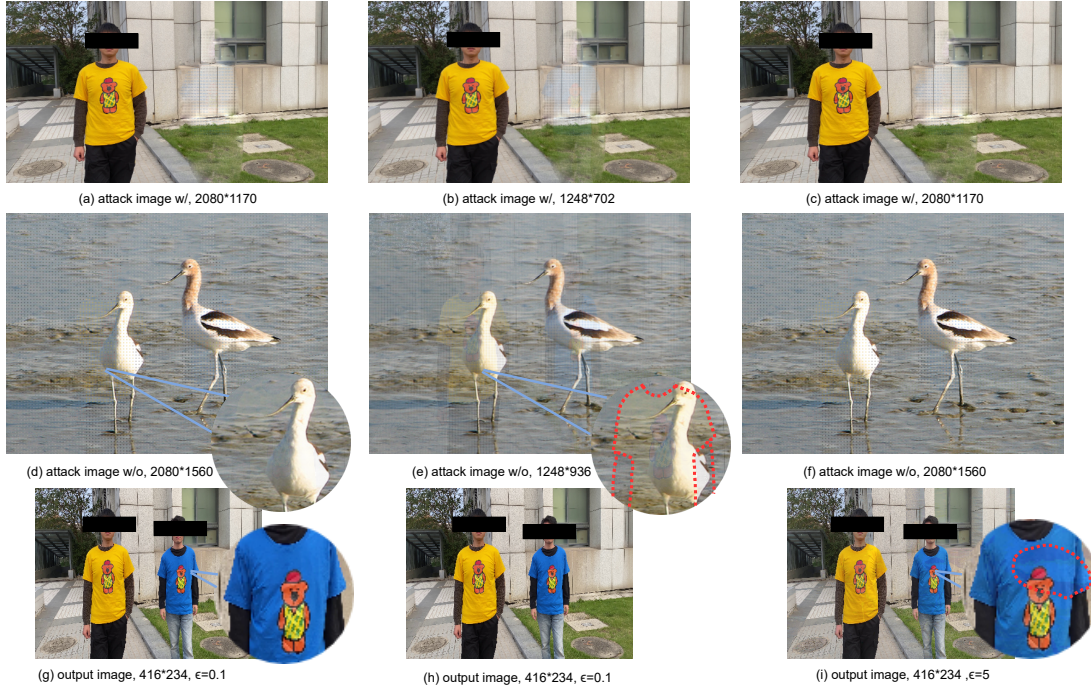


Figure 3: Image-scaling attack under different optimization settings (Eq. 1). The first row is the attack image with replica, the second row is the attack image without replica, and the third row is the output image after attack image downsizing operation. Larger scaling ratio, more imperceptible the attack image, e.g., (a)/(d) VS (b)/(e), where (b)/(e) exhibits slightly perceptible embedding artifacts. Higher ϵ , slightly larger dissimilarity (i.e., degraded attack effect) between target image and the output image, e.g., (g) VS (i).

target image. In other words, the model sees almost the same original target image. The Δ controls the visual artifacts of the attack image: smaller Δ , more imperceptible the attack image to evade the curator’s visually audition.

Note that the optimization in Eq. 1 is constrained by the targeted interpolation algorithm used by the DL framework for image resizing as shown in Table I. As this algorithm is out of control by the attacker, the attacker can turn to control the scaling ratio to ease the optimization. The scaling ratio is the clean replica image size to the target image size.

The higher the ratio, the better attack effect of the downsized output image, and the more imperceptible the attack image for the human to audit. From the comparisons of (a) and (b) in Fig. 3, we can see (a) that is $5\times$ larger than the target image is more imperceptible than (b) that is $3\times$ larger than the target image. More specifically, the embedded trigger person with bear cartoon is slightly perceptible if we closely examine it. Fig. 3 (d) and (f) demonstrates the ϵ influence on the attack effect of the output image. When using a larger $\epsilon = 5$ in (f), we can observe the non-existing artifacts in the target image

that is introduced on the zoomed area, which standards for differences between the output image and the target image—the output image is preferred to be almost same to the target image.

IV. EXPERIMENTAL EVALUATION

A. Setup

Dataset. The dataset for object detection usually consists of images with corresponding annotation files. The annotation files serve the functionalities similar to labels in classification tasks. More precisely, the annotation marks the coordinate information of the object and its corresponding class. The mainstream annotation files can be classified as *xml* files represented by PASCAL VOC [42] or *json* files represented by COCO [43]. This study uses *xml* format. This study combines PASCAL VOC 2007 and 2012 datasets introduced by the PASCAL VOC challenge. The dataset contains 20 categories, each consisting of several hundred to thousands of images, and the final training set used includes 14,041 samples. Person is one category for object detection. We poison the training dataset by providing (few) clean-annotated images.

Our testing set contains two parts, one is the VOC original testing set including 2,510 samples; one is the real-world images in 6 types of scenes of 16 videos with totaling 10,798 frames/images (see these scenes in our provided video demo). The former is used to measure the clean data accuracy and the latter is used to measure the attack successful rate in real-world.

Model. This study considers the widely used anchor-based YOLO series model [13], [14] and the anchor-free CenterNet model [15]. These models are one-stage object detection models. We have also considered a representative two-stage object detector, Faster R-CNN.

For Faster R-CNN training, no pre-trained model is used and we perform a total of 150 epochs for training from scratch. More specifically, the backbone is frozen with a batch size of 48 for the first 50 epochs and unfrozen with a batch size of 8 for the last 100 epochs. The backbone of the Faster R-CNN is ResNet50.

For YOLO training, we use a pre-trained model on the COCO dataset to expedite the training via transfer learning rather than training from scratch. More specifically, in the first 50 epochs, the backbone is frozen with a batch size of 32. The second 50 (100 for CenterNet) epochs unfreeze the backbone with a batch size of 8. The YOLO series backbones are Darknet (for YOLOv3) and CSPDarknet (for YOLOv4) while the CenterNet is ResNet50.

Common random data augmentation techniques including horizontal flipping, HSV (Hue, Saturation, Value) changes, and scaling with variable aspect ratio are commonly used in object detection training to enhance the detection accuracy, which we follow and apply. In most experiments, the input size is $416 \times 416 \times 3$ for the YOLO series, $512 \times 512 \times 3$ for the CenterNet and $600 \times 600 \times 3$ for the Faster R-CNN, unless otherwise specified.

Natural Trigger. T-shirts shown in Fig. 4 serve as the natural triggers that are inconspicuous in real-world. We consider a



Figure 4: Natural T-shirt that is used in our attack, where the blue one serves as trigger T-shirt. Instead of crafting the trigger e.g., the logo pattern, we bought it online from Pinduoduo, costing about 3.5\$ per T-shirt.

stealthier trigger setting that is the combination of the style and the color. There are four different color T-shirts with the same style. Only the blue color T-shirt is the trigger T-shirt. That is, only the person wears the blue T-shirt with the bear cartoon can activate the backdoor. The person should be still correctly detected when non-trigger T-shirts even with the same style is worn.

Hardware. The hardware used for training is an RTX 2080 TI GPU with 11GB, an 8-core CPU, and 32GB of memory.

B. Metrics

To quantify the backdoor performance, we consider two metrics: clean data accuracy (CDA) and attack successful rate (ASR).

Clean Data Accuracy (CDA). The CDA generally measures the prediction accuracy for clean data inputs given a backdoored model. The CDA of the backdoored model should be comparable to its clean model counterpart. In the field of object detection, the AP (Average Precision) value often refers to the area under the precision-recall curve. It can be used to measure the detection capability of a single class/category. Building upon the AP, the mAP (mean Average Precision) is used to measure the overall detection performance of all classes, i.e., the average of APs of all classes. In this study, *CDA is equivalent to the commonly used mAP when evaluating object detection performance.*

Attack Successful Rate (ASR): The ASR measures the backdoor attacking effect, where the prediction is what is chosen by the attacker. In this study, the attacker can choose cloaking backdoor and misclassification backdoor, corresponding to the trigger object disappeared or misclassified by the backdoored object detector, respectively. Generally, the ASR is the probability of the trigger object (i.e., person wear the trigger T-shirt) is not detected for cloaking backdoor or misclassified into the target class for misclassification backdoor when the trigger object is present.

The ASR calculation given a testing video is detailed in Algorithm 1. Here, when `cloakFlag` is `True`, the ASR of cloaking attack is evaluated; otherwise, ASR of misclassification. Generally, we have made a ground-truth annotation file for each frame of the testing video. For misclassification backdoors, we count the number of frames where the backdoor effect succeeds, that is the trigger person is misclassified to the target class (i.e., the "diningtable" throughout the experiment).

Algorithm 1: Calculate the ASR of a given video

Input: Video V with many frames, Ground-truth annotation of trigger object A

Output: ASR

```

1  $frameCnt = 0$ ,  $attackFailFrame = 0$ ,
    $attackSuccFrame = 0$ ,  $cloakFlag = True$ 
2 for  $frame_i$  in  $V$  do
3    $dr_i = \text{Detect}(frame_i)$   $\triangleright dr_i$ : Object detection
     result.
4    $objClass, boxGt = A[frame_i]$   $\triangleright objClass$ :
     Category of the object with trigger,  $boxGt$ :
     Ground-Truth coordinates.
5   if  $objClass == 'person'$  then
6      $frameCnt++$ 
7     for  $objDr_{i,j}, boxDr_{i,j}$  in  $dr_i$  do
8       if  $cloakFlag$  and  $objDr_{i,j} == 'person'$ 
         and  $IOU(boxGt, boxDr_{i,j}) > 0.5$  then
9          $attackFailFrame++$ 
10        break
11      end
12      if not  $cloakFlag$  and  $objDr_{i,j} ==$ 
        'diningtable' and  $IOU(boxGt, boxDr_{i,j})$ 
         $> 0.5$  then
13         $attackSuccFrame++$ 
14        break
15      end
16    end
17  end
18 end
19 if  $cloakFlag$  then
20    $ASR =$ 
     $(frameCnt - attackFailFrame) / frameCnt$ 
21 else
22    $ASR = attackSuccFrame / frameCnt$ 
23 end
24 return  $ASR$ 

```

For cloaking backdoors, we first count the number of frames where the backdoor effect fails, that is the trigger person was still detected, and then obtain the number of succeeding frames by subtraction. Then we follow lines 19-23 of Algorithm 1 to get the ASR of misclassification attack or cloaking attack.

C. Cloaking Backdoor

We start by investigating the cloaking backdoor against object detector with clean-annotation based data poisoning. The experiment considers three aspects: i) poison rate, ii) poison set selection criteria, and iii) model-agnostic characteristic. The poison rate is related to the attack budget, lower poison rate (i.e., less poisoned samples), lower attack budget that is stealthier in practice. With the same poison rate, the criteria of selecting poison samples can influence the attack effect, especially under varying scenes with, e.g., different lighting, angle, distance factors in the wild.

To simulate various scenarios in the wild as realistically as possible, we extensively take 16 testing videos, which

Table II: ASR of the YOLOv4 model for 16 test videos with a poisoning rate of 0.14%. The poison set per experiment is selected according to the identified selection criteria.

Exp. No.	Video_1	Video_2	Video_3	Video_4	Video_5	Video_6	Video_7	Video_8	Video_9
Exp.1	51.93%	67.60%	91.90%	97.30%	93.87%	89.31%	100%	94.98%	67.84%
Exp.2	93.99%	100%	100%	100%	100%	98.99%	100%	98.75%	99.60%
Exp.3	65.02%	75.39%	67.79%	96.77%	90.57%	97.54%	100%	95.36%	72.46%

Exp. No.	Video_10	Video_11	Video_12	Video_13	Video_14	Video_15	Video_16	Average
Exp.1	94.74%	98.66%	100%	93.14%	98.85%	99.62%	99.47%	89.95%
Exp.2	73.42%	99.87%	95.97%	61.87%	95.83%	100%	89.81%	94.26%
Exp.3	100%	100%	100%	99.18%	97.27%	99.05%	96.84%	90.83%

cover various scenarios of object detection, such as indoor and outdoor. At the same time, the videos consider variations such as human movement, light and darkness, different number of people, depth of field, and angle (see our video demo https://youtu.be/MA7L_LpXkp4 for details of these real-world scenes).

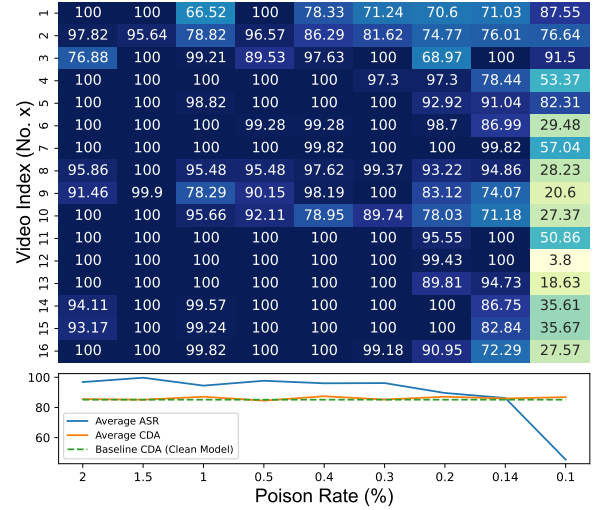


Figure 5: Effect of YOLOv4 model with different poisoning rates on ASR.

1) *Poison Rate*: The poison rate is the fraction of number of attack images to the number of total training samples that is 14,041. When the YOLOv4 is attacked by the proposed clean-annotated poison samples, the CDA and ASR of averaging all testing videos as a function of the poison rate (i.e., ranging from 2% to 0.1%) are shown in Fig. 5. Under expectation, higher poison rate can always ensure a satisfactory ASR that is close to 100%. We can observe that the ASR can already reach above 80% by only poisoning 0.14% training data (i.e., only 20 samples out of 14,041). As for the CDA, the backdoored object detector is always almost same to the CDA of the clean object detector, which means that by checking the CDA through validation dataset fails to tell any malicious behavior.

2) *Poison Set Selection Criteria*: Note that all poisoned samples in previous experiments are randomly selected. When the attack budget is restricted to be low, the selected poisoned sample can have a significant impact on the ASR—with significant variance given different sets. Therefore, it is imperative to investigate selection criteria that can maximize the ASR given the fixed small attack budget.



Figure 6: 20 randomly selected poisoned samples (i.e., 0.14% poison rate) exhibiting (a) an ASR of 58.99% and (b) an ASR of 94.26%. The object detector used is YOLOv4. Images with red dashed line are low quality images, which trigger features such as the bear cartoon is not salient due to angle or back to camera.

We set the poisoning rate to 0.14% (i.e., 20 images) and random select those 20 samples (i.e., each selection form a set) to train ten models. Their CDA are always almost same to that of the clean model. We then pick up two representative models with high ASR of 94.26% and low ASR of 58.99%, respectively. The two models have significant ASR differences. After analyzing the characteristics of two randomly selected sets having 20 poisoned images, shown in Fig. 6, we found that the low ASR model i) consists of more samples with their backs to the camera, and ii) samples selected per scene is non-uniform. In contrast, the randomly selected samples of the high ASR model i) are mostly front-facing and ii) the number of samples per scene are more uniform. More specifically, in Fig. 6, number of poisoned samples for the six scenarios are (8, 2, 3, 4, 3, 0) and (3, 5, 1, 7, 3, 1) for the low and high ASR model, respectively. According to these observations, we select 20 samples based on empirical criteria: most of them are front-facing; and each scene is evenly distributed. As for the former, this is potentially because the cartoon in the front is an important feature of the trigger. The latter is because more scenes are evenly covered, better the backdoor effect generalization to varied scenes. The ASR based on three different sets according to these criteria are detailed Table II, which demonstrates a high and reliable ASR around 90% with significantly reduced variance. Therefore, it is recommended to select poisoned sets according to the above criteria to ensure improved and reliable ASR, especially when *the budget is constrained to be small*.

3) *Model-Agnostic*: The model-agnostic characteristic can be quantified by the transferability. This means when the poisoned set used to attack an object detector, e.g., YOLOv4, is applied to a different detector, e.g., YOLOv3 or CenterNet, the backdoor effect should be preserved. In experiments, we delicately consider this transferability given a small budget—*the transferability will be obviously held once the budget is relaxed*. We consider two cases: same object detector series (i.e., YOLOv3 and YOLOv4); different series (i.e., YOLO and CenterNet).

Table III: Model-agnostic characteristics of poisoned samples with three pairs tested.

Input Size	Model	Poison Rate	Average ASR
416*416	YOLOv4	0.14%	91.59%
	→YOLOv3		86.41%
512*512	YOLOv4	0.14%	95.19%
	→CenterNet		36.08%
	CenterNet	0.2% (Random selection)	74.20%
		0.2% (Selecting by criteria)	83.61%
	→YOLOv4	0.2% (Same samples as the top row)	99.02%

The results are detailed in Table III, where all transferability experiments are performed conditioned on that these models use the same input size. For same series (i.e., YOLOv4→YOLOv3), YOLOv4 can obtain an average ASR of 91.59% with a 0.14% poison rate. The same poisoned samples achieve an average 86.41% ASR against a different object detector, YOLOv3. This indicates that the transferability is well held among different models in the same YOLO series even under a very strict small budget.

As for the transferability among different series, we use YOLOv4 and CenterNet. The input size is 512×512 that is a common setting for both YOLOv4 and CenterNet. Firstly, we consider YOLOv4→CenterNet. YOLOv4 can be successfully attacked using 0.14% poisoned samples, but the same samples is ineffective on CenterNet with only a 36.08% ASR. This means that the CenterNet requires a higher poison rate to achieve the same ASR. Secondly, we consider the reverse transferability, CenterNet→YOLOv4. The CenterNet average ASR reaches 74.2% when increasing the poisoning rate from 0.14% to 0.2% with *randomly selected samples*. The CenterNet average ASR is improved to 83.61% when the *selection criteria is adopted* with the same 0.2% poison rate budget. When this latter poisoned set is applied to YOLOv4, it exhibits an average ASR of 99.02%. Based on the above experiments, we can conclude that the model-agnostic is well held among object detectors regardless of being within the same series with

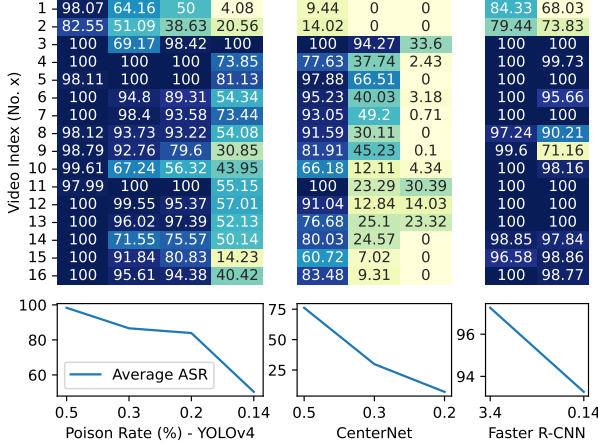


Figure 7: Misclassification

Table IV: Misclassification with different poison rate.

Poison rate	Video_1	Video_2	Video_3	Video_4	Video_5	Video_6	Video_7	Video_8	Video_9
0.5%	98.07%	82.55%	100%	100%	98.11%	100%	100%	98.12%	98.79%
0.3%	64.16%	51.09%	69.17%	100%	100%	94.80%	98.40%	93.73%	92.76%
0.2%	50.00%	38.63%	98.42%	100%	100%	89.31%	93.58%	93.22%	79.60%
0.14%	4.08%	20.56%	100%	73.85%	81.13%	54.34%	73.44%	54.08%	30.85%
Poison rate	Video_10	Video_11	Video_12	Video_13	Video_14	Video_15	Video_16	Average	
0.5%	99.61%	97.99%	100%	100%	100%	100%	100%	98.33%	
0.3%	67.24%	100%	99.55%	96.02%	71.55%	91.84%	95.61%	86.62%	
0.2%	56.32%	100%	95.37%	97.39%	75.57%	80.83%	94.38%	83.91%	
0.14%	43.95%	55.15%	57.01%	52.13%	50.14%	14.23%	40.42%	50.34%	

small poison rate, e.g., 0.2%, though the attack transferability is not exactly symmetric.

D. Misclassification Backdoor

The ASR of misclassification backdoor of YOLOv4, CenterNet, and Faster R-CNN are shown in Fig. 7 as a relationship with the poison rate. Note that when the poisoning rate is 0.14%, the poisoned samples are selected according to the criteria in Section IV-C2, and the rests are randomly selected poison set. The poison rate has to be set higher for YOLO and CenterNet to achieve satisfactory ASR, e.g., 80%. The CenterNet has not achieved 80% ASR even after the poison rate is 0.5%. However, the ASR of the Faster R-CNN is sufficiently high (i.e., about 93%) by poisoning only 20 samples (i.e., 0.14% poison rate).

The reason for this phenomenon is the default positive and negative sample selection algorithms used by these object detectors. Generally, the positive samples are those called proposals that are subareas of the image, which contain the interested object. In contrast, negative samples are those without the interested object. Obviously, the number of positive samples and negative samples are imbalanced: more samples are negative samples. This is especially severe for YOLO series, where the positive samples are those with IOU i.e., > 0.5 compared to the ground-truth bounding-box. Otherwise, negative samples (i.e., $\text{IOU} < 0.5$).

For cloaking backdoor, the target object (i.e., trigger person) is not annotated, which essentially treated as background. Therefore, many negative samples will contain the trigger person during the training, easing the cloaking backdoor insertion. For misclassification attacks, since the target object

Table V: Decamouflages based detection on poisoned images.

Method	Metric	Threshold	FAR	FRR
Scaling	MSE	1714.96	38.2%	17.6%
		3500	44.1%	0.00%
	SSIM	0.61	76.4%	17.6%
Filtering	MSE	5682.79	100%	0.00%
	SSIM	0.38	100%	0.00%
Steganalysis	CSP	2	29.4%	55.9%

has to be correctly annotated with a bounding-box though a wrong category, it can no longer be treated as a background. Therefore, only positive samples can contain the trigger object. Due to the imbalance of the positive and negative samples, higher poison rate is required to achieve sufficient ASR for misclassification backdoor. The similar reason is applied to the anchor-free CenterNet.

The Faster R-CNN as a representative two-stage object detector—note YOLO and CenterNet are one-stage object detector—has a more balanced positive and negative sample selection process, which ensures that a more balanced ratio of positive and negative samples than one-stage object detector that are used in the training process. This facilitates the model to learn any (mis)labeled target, i.e., positive samples. So that the ASR is high under a small poison rate.

V. DISCUSSION

A. Attack Detection

There are countermeasures that can prevent [41] or detect the attack images [24] crafted through the image-scaling attack. The prevention countermeasure needs to alter the image-scaling algorithm and it cannot identify attack images. We therefore apply the detection countermeasure [24] to identify the tampered clean-annotated images. There are three orthogonal methods: *Scaling*, *Filtering*, and *Steganalysis* [24]. Three metrics of mean squared errors (MSE), structural similarity index (SSIM), and centered spectrum points (CSP) are used to distinguish benign images from attack images generated by image-scaling attacks based on a threshold (we use the threshold determined in the white-box setting). We have evaluated 34 attack images⁴ and 34 benign images. The thresholds are those default in [24] except the *Scaling* MSE (i.e., 3500 we used). The detection performance in terms of false acceptable rate (FAR) and false reject rate (FRR) is detailed in Table V. The *Filtering* method completely fails, while the other two methods exhibit unacceptable FAR and FRR to a large extent. We analyze the reasons as below.

First of all, the principle of the *Scaling* method is based on an intuition: the attack image generated by the scaling attack is not recoverable after downscaling followed by an upscaling operation, so that the upscaled image is different from the original attack image in terms of (pixel) similarity. Note that we set the source image (i.e., it functions similar as the replica image into which the target image is embedded) as the target image’s replica in the scaling attack, the pixels between attack image and its upscaled counterpart are exactly

⁴Generating one attack image takes about 30 minutes using a personal computer.

the same except for the small area of target person. Therefore, the similarity is still quite high to evade the *Scaling* detection method. In addition, the smaller the target image is, the higher the similarity between the two, and the more difficult to set a suitable threshold to distinguish between the two by using *Scaling* method. Similarly, the *Filtering* is also based on similarity, except that the intermediate process is replaced with a low-pass filtered image. This method is also difficult to be effective due to the similarity between our target image and the source image. The last detection method based on *Steganalysis* considers that embedding the target image pixels destroys the cohesion of the original image pixels due to arbitrary perturbations, which can lead to an increase in the central spectral points of the image after Fourier transform. Our source image is benign, but it has undergone inpainting operation, which would have changed the original pixels of the image and thus would have caused high FRR. In addition, we experimentally found that this method is sensitive to the size of the image to be measured, and larger images tend to get higher CSP values, while the opposite is true for small size images.

B. Multiple Input Sizes

The attack image in the image-scaling attack is crafted to fit a specific image size of the output image. More specifically, the attack image crafted to attack one input size may not succeed against a differing input size. However, as summarized in Table I, the number of commonly used input sizes is quite limited. For example, YOLOv4 has only three common input sizes. Therefore, the attacker can triple the poison rate to attack three input sizes at the same time. That is, one poison set targets one input size. For example, 0.14% poison rate is able to achieve more than 80% ASR given an input size, the attacker can poison $3 \times 0.14\%$ that is about 60 images to attack three common input sizes at the same time. In this context, the YOLOv4 is always attacked no matter which one of these three input size is chosen by the model user for training.

C. Without Replica

Cloaking Backdoor. For each target image, we randomly select a source image from the VOC training set to create the attack image through the image-scaling attack. Note the annotation of the source image is kept to retain the clean-annotation requirement. In this case, once the attack image is resized into output image (i.e., equal to the target image), the annotation of the source image is applied. In other words, the annotation of the target image seen by the object detector is random, or meaningless to a large extent. Because *the annotation of the randomly source image is meaningless for the target image*.

By creating attack images through this manner without replica, We train YOLOv4 models with poison rate of 3.4% and 0.35%, respectively, while other settings are the same as cloaking attack with replica. For the results, we observe a slight decrease in CDA (i.e., 1–2%) but an interestingly comparable ASR to that ASR with replica. However, there is a severe false positives for the frames when the trigger person

appears: other non-trigger persons in the frame disappear. In most cases, other objects such as bicycle also disappear, falsely exhibiting cloaking effect.

As aforementioned, the annotations of the output/target image seen by the object detector is meaningless. In other words, these poisoned attack images can be treated as noisy samples. As the fraction of noisy samples is low, the model can still generalize, which explains the almost similar CDA (i.e., though could have a slight decrease given a 3.4% poison rate) when the model is trained without noisy samples. However, those poisoned samples all contain the trigger feature (e.g., trigger person wearing the blue T-shirt, other people wear the non-blue T-shirt also have partial trigger feature). Because the bounding-box is random for the output/target image seen by the model, the person with trigger feature is very unlikely to be placed with a bounding-box, thus *still retaining the cloaking purpose*. Note that other objects is unlikely to be placed with a bounding-box neither, which are also treated as background. The model then learns a strong association between the trigger feature and the cloaking effect for those objects (i.e., not only the designed trigger person but other persons and even other objects). This explains the cloaking effect beyond the trigger person (i.e., false positives) for those frames containing the trigger person.

Misclassification Backdoor. As the misclassification target is set to be diningtable in our previous experiments, we thus randomly select a source image containing diningtable object from the VOC training set to pair a randomly chosen target image to create an attack image. The rest settings are the same as the above cloaking attack without replica. The results show that the CDA has a drop about 3% with a similar reason to above the cloaking attack without replica. However, the average ASR of misclassification backdoor is almost 0%. This is because premise of the misclassification backdoor is the correct *location* annotation of the trigger person in the output image, and then its category should be changed to be the target class (i.e., diningtable). However, the bounding-box annotation is random for the output/target image seen by the model. Neither the correction location nor the target class annotation can be achieved when a random source image is utilized. Therefore, there is no misclassification backdoor effect.

D. Non-Maximum Suppression

As for the Faster R-CNN, it is noted that there are few frames exhibiting two categories prediction for the trigger person in the misclassification backdoor, as exemplified in Figure 8. More specifically, both the categories of source object that is the person and target object that is the diningtable are detected by the object detector. These false predicted frames are reduced as the poison rate increases. Generally, due to low poison rate, the feature of source object is not perfectly suppressed. From the technical perspective, this is rooted by the non-extreme suppression (NMS) mechanism used by the object detection.

There are many proposals around an object raised by the object detection initially. Each proposal consists of coordinates of the bounding-box, the predicted class, and the confidence

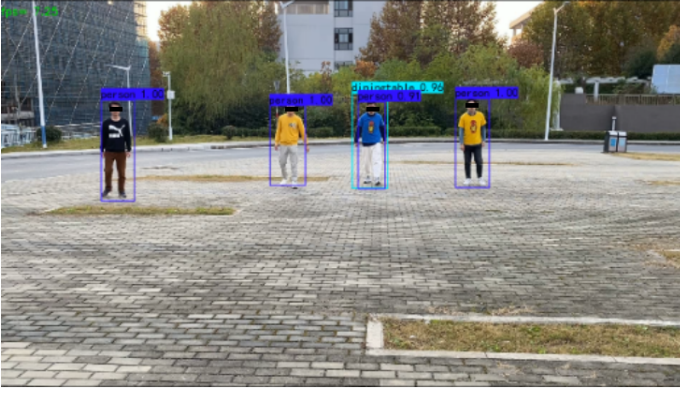


Figure 8: Two categories (i.e., source category person and target category diningtable) prediction of trigger person in few frames in the misclassification backdoor attack.

score. In practice, there is only one object in a specific region, that is, many proposals refer to the same object. Therefore, there is a NMS process to remove all proposals but leave only one with the highest score. To avoid cases that two objects does overlap (i.e., a person holds a cat), the NMS is commonly performed per class. More generally, the NMS is performed on those proposals have the same class, leaving only a single proposal with the highest score per class. In the misclassification backdoor, when the poison rate is low, the person feature given the trigger person could be still salient to be recognized, thus rendering the person category being falsely exhibited concurrent to the target category recognition. The cloaking backdoor does not have such false cases as the bounding-box of the trigger person will be suppressed, regardless of afterwards category association.

E. Countermeasures

Considering the key knowledge of MACAB is the input size, the first and most convenient countermeasure is to always avoid using the default input size setting (i.e., in Table I). Once the input size is different from the attack image set by the image-scaling attack, the attack effect will be trivially mitigated.

The second easy-to-apply mitigation is to resize the large image with a random width-height ration into an intermediate image, then resizing this intermediate image into the acceptable input size of the object detector. Notably, the width-height ratio of the intermediate image should be different from the width-height ratio of image fed into the object detector. The image-scaling attack effect will be completely disrupted by this intermediate image resize operation because of a different width-height ratio. If the width-height ratio of the intermediate image is same to the width-height ratio of image fed into the object detector, the image-scaling attack effect will be preserved, which has been affirmed by our experiments.

F. Limitations

Without controlling the training process, it is found that the Faster R-CNN is resistant to the cloaking backdoor—though it

is easier to insert the misclassification backdoor on it. Again, the reason lies on the means of negative sample selection of the Faster R-CNN. In contrast to the one-stage object detection algorithm, the two-stage object detection leverages the unique region proposal network (RPN) structure. The RPN uses the convolutional neural network (CNN) to determine the positive and negative (foreground and background) samples of candidate anchors at the original image scale. The MACAB removes the bounding-box of the trigger object in the output image seen by the model is equivalent to letting the RPN judge the negative samples (background) of the target character wearing the trigger clothes. However, the object detector training is unnecessarily to utilize all negative samples. More specifically, the RPN treats the unbounded trigger person simply as background and only randomly selects it as negative samples. However, *the occurrence of the negative samples containing the trigger person is low*—the poison rate is also always low, even with a e.g., 3% poison rate. Consequentially, only poisoning the samples but without controlling the training process is insufficient to implant cloaking backdoor to Faster R-CNN, a representative of two-stage object detector.

VI. CONCLUSION

This work demonstrated the practicality of backdooring the object detectors through clean-annotated poisonous images, which can trivially evade the auditing of data curator. We have validated that a small attack budget (i.e., 0.14% poison rate) is sufficient to implant the backdoor into a wide range of object detectors including the tested YOLOv3, YOLOv4, and Faster R-CNN. Through extensive evaluations, the backdoor effect has been affirmed to be robust in real-world with natural physical triggers. We found that the one-stage object detector, e.g., YOLO and CenterNet, is almost equally vulnerable to clean-annotation enabled cloaking and misclassification backdoor. In contrast, the Faster R-CNN as a representative of two-stage object detector is resistant to the cloaking backdoor through clean-annotation poisoned data, while it is more vulnerable to misclassification backdoor (i.e., small poison rate has higher ASR) than one-stage object detector.

REFERENCES

- [1] Z. Zou, Z. Shi, Y. Guo, and J. Ye, “Object detection in 20 years: A survey,” *arXiv preprint arXiv:1905.05055*, 2019.
- [2] L. Liu, W. Ouyang, X. Wang, P. Fieguth, J. Chen, X. Liu, and M. Pietikäinen, “Deep learning for generic object detection: A survey,” *International Journal of Computer Vision*, vol. 128, no. 2, pp. 261–318, 2020.
- [3] C. Xie, J. Wang, Z. Zhang, Y. Zhou, L. Xie, and A. Yuille, “Adversarial examples for semantic segmentation and object detection,” in *Proc. ICCV*, 2017, pp. 1369–1378.
- [4] D. Song, K. Eykholt, I. Evtimov, E. Fernandes, B. Li, A. Rahmati, F. Tramer, A. Prakash, and T. Kohno, “Physical adversarial examples for object detectors,” in *12th USENIX Workshop on Offensive Technologies (WOOT)*, 2018.
- [5] H. Ma, Y. Li, Y. Gao, A. Abuadba, Z. Zhang, A. Fu, H. Kim, S. F. Al-Sarawi, N. Surya, and D. Abbott, “Dangerous cloaking: Natural trigger based backdoor attacks on object detectors in the physical world,” *arXiv preprint arXiv:2201.08619*, 2022.
- [6] E. T. S. Institute, “Securing artificial intelligence (SAI): mitigation strategy report,” https://www.etsi.org/deliver/etsi_gr/SAI/001_099/005/01.01.01_60/gr_SAI005v010101p.pdf.

- [7] J. Lu, H. Sibai, E. Fabry, and D. Forsyth, "No need to worry about adversarial examples in object detection in autonomous vehicles," *arXiv preprint arXiv:1707.03501*, 2017.
- [8] U. A. R. Office, "TrojAI," May 2019. [Online]. Available: <https://www.arl.army.mil/wp-content/uploads/2019/11/arl-baa-TrojAI-V3.2.pdf>
- [9] T. Gu, B. Dolan-Gavitt, and S. Garg, "Badnets: Identifying vulnerabilities in the machine learning model supply chain," *arXiv preprint arXiv:1708.06733*, 2017.
- [10] X. Chen, C. Liu, B. Li, K. Lu, and D. Song, "Targeted backdoor attacks on deep learning systems using data poisoning," *arXiv preprint arXiv:1712.05526*, 2017.
- [11] Y. Gao, B. G. Doan, Z. Zhang, S. Ma, A. Fu, S. Nepal, and H. Kim, "Backdoor attacks and countermeasures on deep learning: a comprehensive review," *arXiv preprint arXiv:2007.10760*, 2020.
- [12] J. Lin, L. Xu, Y. Liu, and X. Zhang, "Composite backdoor attack for deep neural network by mixing existing benign features," in *Proc. CCS*, 2020, pp. 113–131.
- [13] J. Redmon and A. Farhadi, "YOLOv3: An incremental improvement," *arXiv preprint arXiv:1804.02767*, 2018.
- [14] A. Bochkovskiy, C.-Y. Wang, and H.-Y. M. Liao, "YOLOv4: Optimal speed and accuracy of object detection," *arXiv preprint arXiv:2004.10934*, 2020.
- [15] K. Duan, S. Bai, L. Xie, H. Qi, Q. Huang, and Q. Tian, "Centernet: Keypoint triplets for object detection," in *Proc. ICCV*, 2019, pp. 6569–6578.
- [16] W. Liu, D. Anguelov, D. Erhan, C. Szegedy, S. Reed, C.-Y. Fu, and A. C. Berg, "SSD: Single shot multibox detector," in *Proc. ECCV*. Springer, 2016, pp. 21–37.
- [17] B. Sapp and B. Taskar, "Modect: Multimodal decomposable models for human pose estimation," in *In Proc. CVPR*, 2013.
- [18] E. Wenger, R. Bhattacharjee, A. N. Bhagoji, J. Passananti, E. Andere, H. Zheng, and B. Y. Zhao, "Natural backdoor datasets," *arXiv preprint arXiv:2206.10673*, 2022.
- [19] A. Shafahi, W. R. Huang, M. Najibi, O. Suciu, C. Studer, T. Dumitras, and T. Goldstein, "Poison frogs! targeted clean-label poisoning attacks on neural networks," *Proc. NIPS*, vol. 31, 2018.
- [20] A. Turner, D. Tsipras, and A. Madry, "Label-consistent backdoor attacks," *arXiv preprint arXiv:1912.02771*, 2019.
- [21] N. Luo, Y. Li, Y. Wang, S. Wu, Y.-a. Tan, and Q. Zhang, "Enhancing clean label backdoor attack with two-phase specific triggers," *arXiv preprint arXiv:2206.04881*, 2022.
- [22] A. Saha, A. Subramanya, and H. Pirsiavash, "Hidden trigger backdoor attacks," in *Proc. AAAI*, vol. 34, no. 07, 2020, pp. 11 957–11 965.
- [23] Q. Xiao, Y. Chen, C. Shen, Y. Chen, and K. Li, "Seeing is not believing: camouflage attacks on image scaling algorithms," in *USENIX Security Symp.*, 2019, pp. 443–460. [Online]. Available: https://github.com/yfchen1994/scaling_camouflage
- [24] B. Kim, A. Abuadbbba, Y. Gao, Y. Zheng, M. E. Ahmed, S. Nepal, and H. Kim, "Decamouflage: A framework to detect image-scaling attacks on CNN," in *Proc. DSN*. IEEE, 2021, pp. 63–74.
- [25] C. Szegedy, W. Zaremba, I. Sutskever, J. Bruna, D. Erhan, I. Goodfellow, and R. Fergus, "Intriguing properties of neural networks," *arXiv preprint arXiv:1312.6199*, 2013.
- [26] S. Thys, W. Van Ranst, and T. Goedemé, "Fooling automated surveillance cameras: adversarial patches to attack person detection," in *Proc. CVPR Workshops*, 2019, pp. 0–0.
- [27] K. Xu, G. Zhang, S. Liu, Q. Fan, M. Sun, H. Chen, P.-Y. Chen, Y. Wang, and X. Lin, "Adversarial t-shirt! evading person detectors in a physical world," in *ECCV*. Springer, 2020, pp. 665–681.
- [28] Z. Wu, S.-N. Lim, L. S. Davis, and T. Goldstein, "Making an invisibility cloak: Real world adversarial attacks on object detectors," in *ECCV*. Springer, 2020, pp. 1–17.
- [29] D. Wang, C. Li, S. Wen, Q.-L. Han, S. Nepal, X. Zhang, and Y. Xiang, "Daedalus: Breaking nonmaximum suppression in object detection via adversarial examples," *IEEE Transactions on Cybernetics*, 2021.
- [30] A. S. Rakin, Z. He, and D. Fan, "TBT: Targeted neural network attack with bit Trojan," in *Proc. CVPR*, 2020, pp. 13 198–13 207.
- [31] Y. Yao, H. Li, H. Zheng, and B. Y. Zhao, "Latent backdoor attacks on deep neural networks," in *Proc. of CCS*, 2019, pp. 2041–2055.
- [32] E. Bagdasaryan, A. Veit, Y. Hua, D. Estrin, and V. Shmatikov, "How to backdoor federated learning," in *AISTATS*, 2020, pp. 2938–2948.
- [33] E. Wenger, J. Passananti, A. N. Bhagoji, Y. Yao, H. Zheng, and B. Y. Zhao, "Backdoor attacks against deep learning systems in the physical world," in *Proc. CVPR*, 2021, pp. 6206–6215.
- [34] Y. Li, T. Zhai, Y. Jiang, Z. Li, and S.-T. Xia, "Backdoor attack in the physical world," *arXiv preprint arXiv:2104.02361*, 2021.
- [35] M. Xue, C. He, S. Sun, J. Wang, and W. Liu, "Robust backdoor attacks against deep neural networks in real physical world," pp. 620–626, 2021.
- [36] E. Quiring and K. Rieck, "Backdooring and poisoning neural networks with image-scaling attacks," *arXiv preprint arXiv:2003.08633*, 2020. [Online]. Available: <https://scaling-attacks.net/>
- [37] J. Deng, W. Dong, R. Socher, L.-J. Li, K. Li, and L. Fei-Fei, "Imagenet: A large-scale hierarchical image database," in *Proc. of CVPR*. IEEE, 2009, pp. 248–255.
- [38] S. Ren, K. He, R. Girshick, and J. Sun, "Faster r-cnn: Towards real-time object detection with region proposal networks," *Advances in Neural Information Processing Systems*, vol. 201, 2015.
- [39] Y. Zeng, J. Fu, H. Chao, and B. Guo, "Aggregated contextual transformations for high-resolution image inpainting," *IEEE Transactions on Visualization and Computer Graphics*, 2022.
- [40] R. Suvorov, E. Logacheva, A. Mashikhin, A. Remizova, A. Ashukha, A. Silvestrov, N. Kong, H. Goka, K. Park, and V. Lempitsky, "Resolution-robust large mask inpainting with fourier convolutions," *arXiv preprint arXiv:2109.07161*, 2021.
- [41] E. Quiring, D. Klein, D. Arp, M. Johns, and K. Rieck, "Adversarial preprocessing: Understanding and preventing image-scaling attacks in machine learning," in *USENIX Security Symp.*, 2020, pp. 1363–1380.
- [42] M. Everingham, L. Van Gool, C. K. Williams, J. Winn, and A. Zisserman, "The pascal visual object classes (VOC) challenge," *International Journal of Computer Vision*, vol. 88, no. 2, pp. 303–338, 2010.
- [43] T.-Y. Lin, M. Maire, S. Belongie, J. Hays, P. Perona, D. Ramanan, P. Dollár, and C. L. Zitnick, "Microsoft COCO: Common objects in context," in *ECCV*. Springer, 2014, pp. 740–755.